

# COMMISSIONING OF A 1.3-GHZ DEFLECTING CAVITY FOR PHASE SPACE EXCHANGE AT THE ARGONNE WAKEFIELD ACCELERATOR\*

M. Conde<sup>1</sup>, H. Chen<sup>2</sup>, W. Gai<sup>1</sup>, C. Jing<sup>1,3</sup>, R. Konecny<sup>1</sup>, W. Liu<sup>1</sup>, D. Mihalcea<sup>4</sup>,  
P. Piot<sup>4,5†</sup>, J. G. Power<sup>1</sup>, M. Rihaoui<sup>4</sup>, J. Shi<sup>2</sup>, Z. Yusof<sup>1</sup>

<sup>1</sup> High-Energy-Physics Division, Argonne National Laboratory, Lemont, IL 60439, USA

<sup>2</sup> Engineering Physics Department, Tsinghua University, China

<sup>3</sup> Euclid TechLabs, Solon, Ohio 44139, USA

<sup>4</sup> Department of Physics, Northern Illinois University, DeKalb, IL 60115, USA

<sup>5</sup> Accelerator Physics Center, Fermi National Accelerator Laboratory, Batavia, IL 60510, USA

## Abstract

A 1/2-1-1/2 cell normal-conducting 1.3-GHz deflecting cavity was recently installed at the Argonne Wakefield Accelerator. The cavity will eventually be included in a transverse-to-longitudinal phase space exchanger that will eventually be used to shape the current profile of AWA electron bunches in support of dielectric wakefield experiments with enhanced transformer ratio. In this paper we report on the initial commissioning of the deflecting cavity including rf-conditioning and beam-based measurement of the deflecting strength.

## INTRODUCTION

Deflecting cavities have found an increasing number of applications in accelerators including particle-species separation [1], beam switchyards [2], longitudinal phase space characterization [3, 4, 5] and advanced phase space manipulations [6, 7]. At the Argonne Wakefield Accelerator (AWA) [8] plans are underway to develop a transverse-to-longitudinal phase-space-exchanger (PEX) beamline [9, 10] and explore its applications to enhance the performances of collinear beam-driven dielectric-wakefield acceleration. Ultimately, this PEX beamline will be used to tailor the current profile of the drive bunch in order to maximize the transformer ratio [11, 12, 13].

A possible configuration for a PEX beamline consists of a transverse-deflecting cavity (TDC) flanked by two dispersive sections arranged as doglegs [9, 10, 14]. The TDC is nominally operated at the zero-crossing phase of the field so that the head and tail of the bunch are subject to opposite transverse momentum kicks. The induced shearing and dispersion occur in the same plane (taken to be the horizontal plane henceforth). The TM<sub>110</sub>-like TDC operates at 1.3 GHz and consists of 1/2-1-1/2 cells; see Fig. 1. The choice of the TDC cells geometry was motivated by the minimization of the beam's centroid motion at zero-crossing operation [15].

\* This work was supported by DOE awards FG-02-08ER41532 with Northern Illinois University, DE-AC02-06CH11357 with Argonne National Laboratory, and DE-SC0006301 with Euclid TechLabs, LLC.

† piot@nicadd.niu.edu

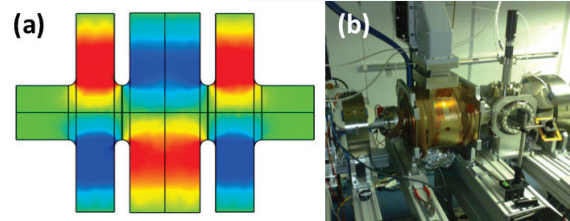


Figure 1: Geometry (a) and picture (b) of the 1.3-GHz TM<sub>110</sub>-like TDC. The superimposed false-color pattern represents the value of the  $E_z$  field in the  $(x = 0, y, z)$  plane (the blue and red colors respectively correspond to the maximum and minimum values of the field).

## EXPERIMENTAL SETUP

As a first step toward building the PEX beamline, only the upstream dogleg and a transverse deflecting cavity (TDC) were installed [17]. The TDC was oriented to deflect (and/or shear) the beam along the vertical direction while the dogleg disperses the beam horizontally. This setup provides a single-shot LPS diagnostic while enabling the commissioning and characterization of the key components necessary for the PEX beamline; see Fig. 2. The main diagnostics used for the results presented below is a Cerium-doped Yttrium Aluminum Garnet (YAG) screen located at a distance  $L = 0.63$  m downstream of the TDC's center.

The cavity was powered with a newly commissioned 30-MW klystron (klystron 2) while the other AWA radiofrequency (rf) components (the rf gun and one pi/2 18-cell booster cavity) were powered with the nominal 25-MW klystron (klystron 1). For the set of measurements reported below, the beam energy and charge were respectively  $E \simeq 14.6$  MeV and  $\sim 1$  nC.

## CAVITY CHARACTERIZATION

Electromagnetic simulations of the cavity carried with CST MICROWAVE STUDIO [18], indicate that the deflecting voltage  $V_{\perp}$  (in MV) scales with the input power  $P$  (in MW) as

$$V_{\perp} = 3.4 \times (P/4.2)^{1/2}. \quad (1)$$

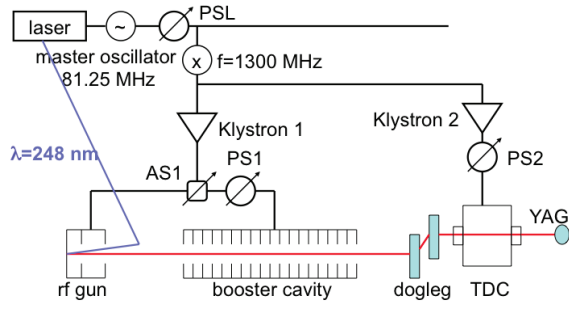


Figure 2: Overview of the experimental setup and associated radiofrequency distribution system. PSL, PS1 and PS2 are variable phase shifters. AS1 is a variable power splitter. The YAG scintillating screen is the main diagnostic used for characterizing the transverse-deflecting cavity (TDC).

For beam dynamics consideration, the deflecting cavity operating at zero crossing is often characterized by its normalized deflecting strength  $\kappa \equiv \frac{eV_{\perp}}{pc} \frac{2\pi}{\lambda}$  where  $e$ ,  $c$ ,  $p$  and  $\lambda$  are respectively the electronic charge, the light velocity, the beam mean momentum and the wavelength of the deflecting mode. In the thin-lens approximation the divergence  $\Delta y'$  and fractional momentum  $\Delta\delta$  changes due to the TDC operated at the zero-crossing phase are related to the initial longitudinal  $z_0$  and vertical  $y_0$  position referenced with respect to the bunch's barycenter via

$$\Delta y' = \kappa z_0, \text{ and } \Delta\delta = \kappa y_0.$$

For the initially intended location of PEX beamline (at  $\sim 15$  MeV), a value of  $\kappa \simeq 3 \text{ m}^{-1}$  was required.

During the rf commissioning, the TDC was powered with forward power exceeding 4 MW without significant processing time. Such a forward power corresponds to a maximum deflecting voltage  $\hat{V}_{\perp} = 3.3$  MV which would result in  $\kappa \simeq 6 \text{ m}^{-1}$  at 15 MeV, a value exceeding our requirement.

A first set of beam-based characterization of the TDC explored the induced vertical deflection impressed on the beam as the phase shifter PS2 is varied. The beam position on the downstream YAG screen is expected to vary as  $\Delta y = L \frac{eV_{\perp}}{pc} \sin(\phi - \phi_0)$ , where  $L$  is the distance from the TDC center to YAG screen and  $\phi_0$  the zero-crossing phase. The measurement confirms this dependency as shown in Fig. 3. This measurement use a klystron 2 forward power of  $\simeq 130$  kW to insure the beam remains within the YAG screen aperture for the maximal induced deflection.

For most of the anticipated applications of the TDC at AWA, longitudinal-phase-space diagnostics and phase space manipulation, the TDC will be operated at the zero-crossing phase thereby resulting in shearing of the beam without a net deflection of the beam's centroid. We therefore performed beam-based measurement of the normal-

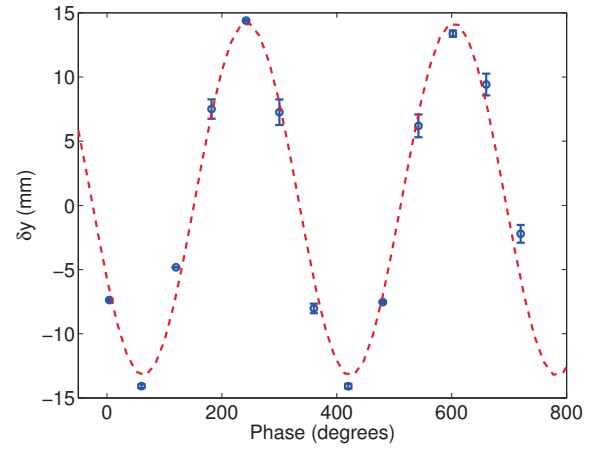


Figure 3: Observed displacement (blue circle with error bars) on the YAG screen as a function of PS2 phase shift. The zero-crossing phases are located at  $\phi_{0,n} = (-23.5 + 180n)^{\circ}$  where  $n = 1, 2, 3, \dots$ . The forward power was set to  $P \simeq 130$  kW. The dashed line is the result of a data fit to a  $A \sin(\phi)$  function.

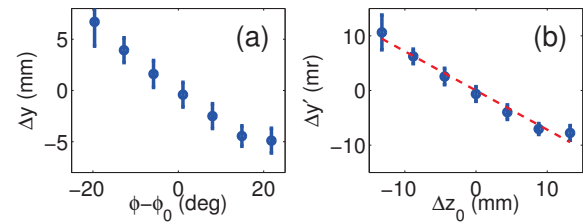


Figure 4: Measured vertical position as function of PS2 phase change around the zero-crossing phase ( $\phi_0$ ) (a) and associated deflection  $\Delta y' \equiv \Delta y/L$  as a function of longitudinal position change (b). The dashed line represents a linear regression of the data and its slope provide the normalized deflecting kick (here  $|\kappa| = 0.72 \text{ m}^{-1}$ ). The forward power is  $P = 20$  kW.

ized deflecting strength as follows. One of the zero-crossing phases  $\phi_0$  is first found, the phase shifter PS2 is then varied around  $\phi_0$ , typically  $\phi \in [\phi_0 - 20^{\circ}, \phi_0 + 20^{\circ}]$ , and the associated beam vertical positions are recorded. For such a small phase variations the change in vertical position writes  $\Delta y \simeq L \frac{eV_{\perp}}{pc} (\phi - \phi_0) \simeq \kappa L z_0$  where  $z_0 \equiv \lambda(\phi - \phi_0)/(2\pi)$  is the longitudinal position at the TDC entrance. Therefore the measurement of  $\Delta y$  for a known variation of  $\phi$  around  $\phi_0$  along with the knowledge of the beam's energy provides an indirect measurement of  $\kappa$ .

The sequence of measurement and data analysis performed for a 20-kW forward power appears in Fig. 4 and a summary of the measured  $\kappa$  values for different forward powers is compared to the simulations in Fig. 5. The measurements are in reasonable agreement with the expected scaling law especially given the large uncertainty on the forward power measurement.

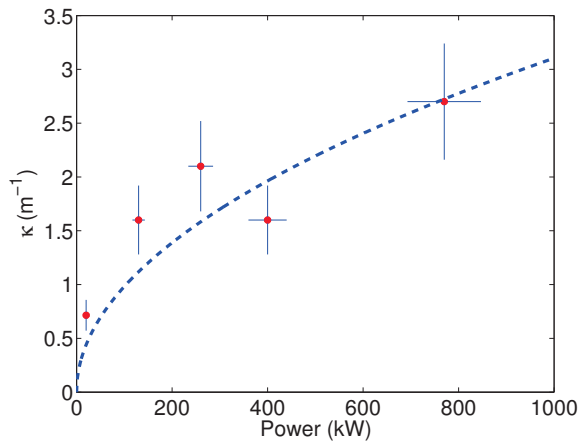


Figure 5: Measured normalized deflecting strength  $\kappa$  as a function of klystron 2 forward power. The dashed line corresponds to the simulation scaling obtained from MICROWAVE STUDIO.

Finally, the TDC was used to carry single-shot longitudinal phase space measurements. Unfortunately our experiment was limited by the rather long bunch ( $\sim 2$  mm for  $\sim 1$  nC) which prevented us from using large deflecting strength without having a large fraction of the beam population outside the YAG aperture; see Ref. [17] for details.

## OUTLOOK

Since our experiments and initial plan for installation of a PEX beamline at AWA, the facility was upgraded and will eventually produce a 70-MeV beam. It is therefore relevant to discuss whether the cavity commissioned using a 14.6-MeV beam can be used in a possible PEX beamline design at 70-MeV. In a PEX beamline a full phase space exchange require the dispersion function  $\eta$  at the TDC location to satisfy

$$\kappa = -1/\eta. \quad (2)$$

Figure 6 displays the required input power as a function of the dispersion at the cavity location for two beam energies (15 MeV and 70 MeV). The cavity was conditioned for input powers in excess of  $\sim 4$  MW so we constraint the input power to a maximum value of 5 MW. Although, the TDC cavity can most probably operate at higher powers, the 5-MW value is driven by the available rf power and its sharing with other critical components. Given this limitation, the scaling provided by Eq. 1, and the required condition for full phase-space exchange Eq. 2, dispersion values larger than  $\sim 0.7$  m are needed at the cavity location. It should finally be pointed out that the required dispersion constrains the maximum tolerable total rms fractional momentum spread for the drive bunch to be limited to  $\sigma_\delta \leq \frac{\lambda}{2\pi\eta}$ . As an example, a large dispersion value of  $\sim 1$  m, would limit  $\sigma_\delta \leq 4\%$  and particles with fractional momentum offset beyond this limit would experience nonlinear effects in the cavity due to the non-uniformity of the

transverse magnetic field for large offsets and corresponding nonlinear variation of the axial electric field.

The design of PEX beamline with dipole magnets with moderate bending angles ( $\sim 20^\circ$ ) providing an enhanced dispersion value at the cavity location have been explored. The two investigated configuration, dogleg- and chicane-based PEXs, can accommodate the TDC with performances described in this paper.

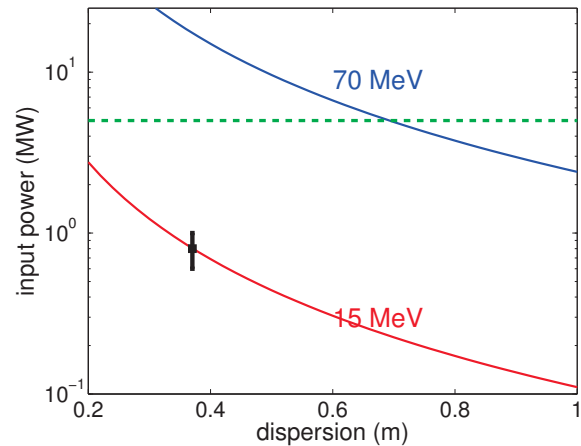


Figure 6: Required power as a function of dispersion at the cavity location for 15 (red) and 70-MeV (blue) beam energies. The data point (black error bar) is obtained from a measurement done at 14.6 MeV at AWA. The green horizontal line delineates the 5-MW limit on input power.

## REFERENCES

- [1] D. A. Edwards, Editor, "An RF Separated Kaon Beam from the Main Injector: Superconducting Aspects", Fermilab TM-2060, October 1998.
- [2] C. Hovater, *et al.*, Proceedings of LINAC96, 77 (1996).
- [3] R. Akre, *et al.*, Proceedings of EPAC 2002, 1882 (2002).
- [4] J. T. Moody, *et al.*, Phys. Rev. ST AB **12**, 070704 (2009).
- [5] C. Behrens, *et al.*, Proceedings of FEL09, 599 (2009).
- [6] M. Cornachia, *et al.*, Phys. Rev. ST AB **6** 030702 (2003).
- [7] Y.-E. Sun, *et al.*, Phys. Rev. Lett. **105**, 234801 (2010).
- [8] Information on the Argonne Wakefield Facility are available at <http://gate.hep.anl.gov/awa>.
- [9] Y.-E. Sun, *et al.*, Proceedings of PAC07, 3441 (2007).
- [10] M. Rihaoui, *et al.*, Proceedings of PAC09, 3907 (2009).
- [11] K. L. F. Bane, *et al.*, SLAC-PUB-3662 (1985).
- [12] P. Piot, *et al.*, Phys. Rev. ST AB **14**, 022801 (2011).
- [13] B. Jian, *et al.*, Phys. Rev. ST AB **15**, 011301 (2012).
- [14] P. Emma, *et al.*, Phys. Rev. ST AB **9**, 100702 (2006).
- [15] J. Shi, *et al.*, Nucl. Instr. Meth. **A598**, 388 (2008).
- [16] M. Rihaoui *et al.*, Proceedings of PAC11, 1857 (2011).
- [17] M. Conde *et al.*, contribution WEPPD077, these proceedings (2012).
- [18] MICROWAVE STUDIO is commercially available from Computer Simulation Technologies AG.